Archaeometry **46**, 2 (2004) 171–182. Printed in Great Britain

THE USE OF OPTICAL COHERENCE TOMOGRAPHY FOR MONITORING THE SUBSURFACE MORPHOLOGIES OF ARCHAIC JADES*

M.-L. YANG

Department of Antiquities, National Palace Museum, 221, Section 2, Chih-shan Road, Shih-lin, Taipei, Taiwan, 111 R.O.C.

and C.-W. LU, I.-J. HSU and C. C. YANG

Graduate Institute of Electro-Optical Engineering and Department of Electrical Engineering, National Taiwan University, Taipei, Taiwan, R.O.C.

We demonstrate the use of the Optical Coherence Tomography (OCT) technique for non-invasive scanning of the subsurface morphologies of jade objects. The two-dimensional tomography images show the refractive index or dielectric constant variations in the samples, reflecting their structures. Three samples of archaic jade objects from the Qijia and Liangzhu cultures in China are scanned in order to understand the subsurface morphologies of the naturally whitened jades. Also, two jade objects with artificial treatments (burning) are scanned and compared with the original materials in subsurface structures. In the original objects, the jade materials can generally be quite transparent, such that the backscattering intensity is weak, although the large-scale (tens of microns or larger) subsurface morphology can be clearly observed. After burning, small-scale (smaller than a few microns) structures are formed and the backscattering intensity is enhanced. In this situation, the large-scale structures may be preserved or even newly generated. On the other hand, in an archaic object with natural whitening, small-scale structures are also formed. Hence, the deeper distributions of significant backscattering intensity are observed, when compared with the unwhitened objects. Nevertheless, the large-scale features diminish during the whitening process. With OCT scanning, such differences in subsurface morphology can provide us a valuable reference for authenticating archaic jade objects.

KEYWORDS: ARCHAIC JADE OBJECT, SUBSURFACE MORPHOLOGY, OPTICAL COHERENCE TOMOGRAPHY, SECONDARY ALTERATION

INTRODUCTION

In China, beginning in the late Neolithic period, people employed nephrite and other beautiful stones to fashion personal ornaments or to create ritual objects for worship (Wen and Jing 1996; Wen 1998). Usually, when the owners of jade objects passed away, the objects were interred along with them. Buried for centuries, both the surface and the interior mineralogical structures of the jade objects were gradually altered, resulting in whitening of the surface and the interior.

The whitening phenomenon, known by traditional Chinese antiquarians as 'shou qin (受沁)', was referred to as 'calcification' in the early period of archaic jade research (Laufer 1912;

* Received 9 December 2002; accepted 5 September 2003.

Pelliot 1925; Salmony 1938; Jayne 1940; Loehr and Fitzgerald Huber 1975). In the past two decades, it has been called 'whitening' or 'secondary alteration' by scholars (Lin *et al*. 1996). Archaeologically excavated archaic jades manifest different degrees of whitening phenomenon. Such differences are primarily due to variations in the mineral composition, fabrication process and depositional environments of the jade objects (Huang 2000; Yang 2000).

The whitening phenomenon is one of the most important characteristics that appear on buried archaic jade objects. In China, it has been one of the key indicators for differentiating authentic objects from forgeries for centuries. Artificially whitened jade objects were usually processed with heating or burning to make the surface brighter in colour. With skilful processes for artificial whitening, it is usually difficult to distinguish between a forged jade object and an archaic one on the basis of appearance alone. Fortunately, after the artificial whitening process, the interior structures of jades are expected to be different from those that have undergone natural processes. Therefore, by scanning the subsurface morphologies of jade objects using a non-invasive means, the different whitening processes can be differentiated. Also, with such a scanning result, the authenticity of the objects can be determined.

At present, most examinations of archaic jade rely on analyses of chemical compositions, such as wet chemical analysis, gravimetric analysis, atomic absorption spectroscopy, X-ray fluorescence analysis, electron probe microanalysis, optical spectrography analysis (Zheng 1983, 1986; Wen 1992, 1993, 1994a,b; Douglas 1996; Klein and Hurlbut 1996; Tsien and Tan 1998), optical emission spectrometry, neutron activation analysis, proton-induced X-ray emission (Renfrew and Bahn 1997) and Raman spectroscopy (Xu *et al*. 1996). Some of these are non-invasive, including Raman spectroscopy and optical spectrography analysis, and can provide us with certain useful information for the study of archaic jade. However, none of the aforementioned methods can give us the micron-scale subsurface morphologies of jade objects.

In this paper, we propose to use the technique of Optical Coherence Tomography (OCT) to non-invasively examine the micron-scale subsurface morphologies of archaic jades and to study the whitening process of these objects. Also, forged jade objects are examined for comparison. Briefly, OCT is a method of low-coherence interferometry utilizing the backscattered signals from refractive-index discontinuities inside a sample. It has been used for interface identification in a layered structure (Fercher *et al*. 1988). Early in the 1990s, this technique was proposed for biomedical tomography, and was called OCT because the axial resolution of this tomography method relies on the coherence of the light source being used (Huang *et al*. 1991). Generally speaking, a light source of larger spectral width corresponds to lower coherence. Because the OCT signal originates from the interference fringe pattern of the backscattered light from a sample, lower coherence implies a narrower interference fringe pattern and hence a higher tomography resolution in the depth scanning direction. Nowadays, OCT is widely used for medical diagnosis. Although optical penetration into the human body is shallow (only 1–2 mm), many parts of the human body can be scanned *in vivo* using an OCT system (Izatt *et al*. 1996; Tearney *et al*. 1997; Chen *et al*. 1999). With a controlled optical intensity applied to the human body or other types of sample, OCT can provide two- or three-dimensional non-invasive tomography scanning. Although OCT has been widely used in biomedical diagnosis and other areas, to the best of our knowledge, the application of this technology to geological materials has not been reported.

This paper is organized as follows. In the second section, we introduce the OCT technique and describe the OCT systems that have been built for jade scanning. Then, in the third section, the OCT scanning results of three archaic jade objects are presented to show the general

subsurface structures of naturally whitened jade. In the fourth section, the OCT scanning results of two recently prepared forged objects are shown. The results for the samples before and after burning are compared to demonstrate the differences in the subsurface structures. Such structures are also compared with those of naturally whitened jade. Further discussions about the scanning results and the conclusions are presented in the fifth section.

OPTICAL COHERENCE TOMOGRAPHY

Typically, an OCT system is built with a Michelson interferometer (for a complete OCT system, see Fig. 1). Here, the optical signal from the light source is split into two arms, the reference arm and sample arm. In the sample arm, photons are incident upon the sample without mechanical contact and the backscattered light returns to the beam splitter to combine with the light reflected from the mirror in the reference arm, to form the interference signal. By translating the position of the reflection mirror in the reference arm, interference signals from layers of different depths in the sample can be obtained. In other words, depth scanning is performed. Before light is incident upon the sample, it is focused, with the focal point inside the relevant layer of the sample. The beam spot size at the focal point determines the tomography resolution size in the lateral dimension. Because the optical intensity illuminating the samples is usually quite weak (less than a few microwatts), it will not damage the samples. In particular, OCT scanning is usually quite fast, with a time of less than 1 s for an image measuring 1 mm $\times$ 1 mm. In this situation, photon-induced changes of jade materials do not seem possible.

An OCT system is designed for high axial resolution and high sensitivity in scanning a sample, which is expected to backscatter a very weak optical signal. When photons are incident upon an object, which usually has a microstructure of a random nature, they experience either large-angle strong or small-angle weak scattering before they are backscattered to the OCT system. The photons that experience weak scattering and bear high coherence with the incident light are expected to provide more direct information about the microstructure of the scanned object. The use of interferometry in an OCT system has the advantage of extracting

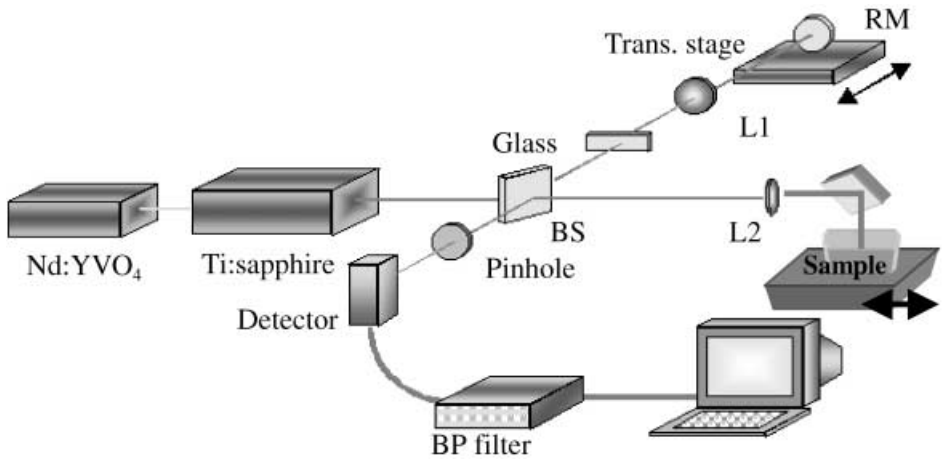

Figure 1 *The layout of OCT system 1. RM, reflection mirror; BS, beam splitter; L1 and L2, lenses; BP filter, band-pass filter.*

only the coherent photons and hence reducing the noise of the system. Therefore, a well-built OCT system can typically have a sensitivity that ranges from 80 to 120 decibels (dB).

Also, because interference can occur only for those optical signals that are backscattered from a thin layer, from which the optical path of the sample arm is about the same as that of the reference arm of the interferometer that is being used, the allowed path length difference is the coherence length of the light source. Therefore, only a thin layer of the coherence length in thickness can be observed with the interferometer at one depth scanning position. In other words, the depth resolution of an OCT system is equal to the coherence length of the light source, which is approximately equal to the inverse of its spectral width. Hence, with a light source of a larger spectral width, a better OCT depth resolution can be achieved (Bouma *et al*. 1996; Hartl *et al*. 2001). The depth resolution, Δz, can be expressed as (Schmitt 1999)

$$\Delta z = \frac{2(\ln 2)\lambda^2}{\pi \Delta \lambda} \tag{1}$$

where λ is the central wavelength and $\Delta\lambda$ is the spectral width of the light source. For instance, with a light source of 800 nm in central wavelength and 100 nm in spectral width, the OCT depth resolution can be as small as 2.8 μm in air when the OCT system is well prepared. Within a scanned object that has a refractive index of 1.65, the resolution becomes 1.7 μm, because the optical wavelength in a material is reduced by the factor of the refractive index. From equation (1), one can see that the depth resolution is proportional to the square of the wavelength. Therefore, a shorter central wavelength results in a better resolution if the spectral width is fixed. However, as mentioned earlier, the incident light experiences scattering within the sample. Such a scattering process would reduce the penetration depth of light for scanning imaging. Typically, the scattering strength is inversely proportional to the fourth power of the wavelength if the microstructure feature sizes are much smaller than the wavelength. Therefore, by using a light source with a longer central wavelength, the scanning penetration depth is larger.

Two OCT systems were built with different light sources for jade scanning. The first system (which will be called system 1 in the following) used a mode-locked Ti:sapphire laser, providing 100 fs, 76 MHz pulses, with the central wavelength at 800 nm. The pulses were coupled into a 5 m single-mode fibre for spectral broadening up to about 50 nm. Therefore, the depth resolution of this system in jade is 3.5 μm, assuming a refractive index of 1.65. The pulses from the output end of the fibre were applied to a free-space Michelson interferometer (see Fig. 1). In the reference arm, a constant-speed translation stage, with a speed of 3 mm s^{-1}, was used for phase modulation and depth scanning. The interference signal was processed using a photodetector and a band-pass filter to extract the image of the subsurface morphology. The lateral resolution of this system is about 5 μm and its sensitivity is over 100 dB.

The second OCT system (system 2) used a Cr:forsterite laser as the light source, which has the central wavelength at 1240 nm and a spectral width of about 30 nm. The spectrum of the laser pulses was broadened up to 65 nm through non-linear optics effects in a 10 m long single-mode optical fibre. The corresponding axial resolution within a jade object is about 7.5 μm. Although the axial resolution is lower compared to that of system 1, the longer central wavelength results in deeper penetration. This OCT system was built with a fibre coupler in order to form the Michelson interferometer. The use of a fibre coupler in an OCT system usually leads to more stable operation. In this OCT system, we built an optical phase delay line in the reference arm for phase modulation and depth scanning (Tearney *et al*. 1997). Compared with the constant-speed translation stage in system 1, the phase delay line can provide a much

higher scanning speed, up to 1000 times higher. The lateral resolution of the second system is also 5 μm. The sensitivity of this system was estimated to be higher than 100 dB.

During the OCT scanning, a jade object was placed on a translation stage, which was connected to a stepping motor for lateral scanning. The distance between the upper surface of the jade object and the focusing lens in the sample arm of the OCT system (L2 in Fig. 1) was in the range of 5–10 mm, depending on the focal length of the lens. Therefore, the jade object was scanned without physical contact. The axial scanning was achieved with operation of a constant-speed translation stage (system 1) or a phase delay line (system 2).

ARCHAIC JADE SAMPLES AND THEIR OCT SCANNING RESULTS

To show the subsurface structures of archaic jade objects with natural whitening processes, we selected three samples, which we have called samples A–C. Sample A came from the Qijia culture (*c*. 2200–1800 BC) near Lanzhou in Gansu Province. Samples B and C belong to the Liangzhu culture (*c*. 3200–2100 BC) in Zhejian Province. The mineralogical properties and origins of the samples used are summarized in Table 1.

In all of the OCT scanning images shown below, the different colour codes represent different backscattering intensities. Because of the scattering—and possibly absorption—in the samples, the backscattering intensity decreases naturally with the scanning depth. However, if there are significant variations in the refractive index within the samples, strong backscattered signals result in clear features in the images. In the images, the white represents the strongest backscattering intensity and the black denotes the weakest signal. In between, the backscattering intensity decreases from red, through orange, yellow, green and blue, to violet. Typically, a sharp white or red curve can be seen in each image, corresponding to the surface of the sample. The colour distributions below this curve describe the subsurface structure of the sample.

Figure 2 (a) shows a photograph of sample A, which is an archaic jade (*Pi*) collected from the Qijia culture. Figure 2 (b) illustrates the OCT scanning image at the indicated white bar in Figure 2 (a) with OCT system 1. In this figure, the signal features above the bright reddish curve, which corresponds to the sample surface, are attributed to the imperfect interference

Table 1 *Sample descriptions*

Sample label	*Sample identification*	*Mineral of sample (identified using Raman scattering)*	*Culture*	*Origin of sample*
A	(NA)	Tremolite (nephrite)	Qijia	Lanzhou (borrowed from Mr Tsai, the collector)
B	K066	Antigorite (serpentine)	Liangzhu	Jiaxing (between Shanghai and Hangzhou), the NPM* collection
C	Tan0201	Antigorite (serpentine)	Liangzhu	Tanshan (near Hangzhou), collection of the first author, MLY
D	JS0207	Tremolite (nephrite)	(NA)	Jiuquan, collection of the first author, MLY
E	FS0105	Tremolite (nephrite)	(NA)	Hangzhou, collection of the first author, MLY

* NPM, National Palace Museum, Taipei.

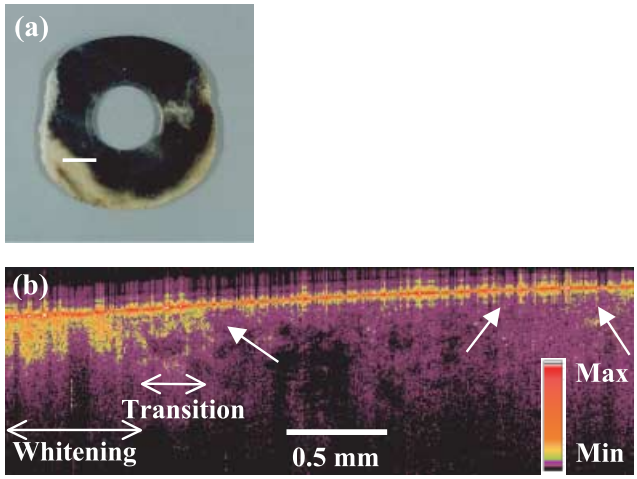

Figure 2 *(a) A photograph of sample A. (b) An OCT scanning image of the sample at a location near the white bar in part (a).*

fringe pattern of the OCT system. Certain weak side-lobes in the interference fringe pattern resulted in the features because of the strong reflection at the surface. Such side-lobes will not affect the demonstration of the subsurface structures in the jade objects. From Figure 2 (b), one can see the micron-scale grain structures (in the order of 100 μm) in the region on the right (the dark portion of the scanned line in Fig. 2 (a)), as indicated with the white arrows. This portion is expected to be less whitened when compared with the whitened portion (the bright portion of the scanned line in Fig. 2 (a)). The OCT scanning image of the strongly whitened portion shows a relatively more uniform and deeper backscattering intensity distribution. Such a backscattering intensity distribution represents the typical feature of the OCT scanning results of strongly whitened jade objects. In Figure 2 (b), the transition region from the weakly whitened portion to the featureless whitened portion can also be recognized.

Figure 3 (a) shows a photograph of sample B, which is a broken jade object from the Liangzhu culture. It had been refashioned in antiquity (in the late Neolithic period) into a jade knife, and had been buried underground for 4000–5000 years. Depending on the extent of the whitening, three surface colours can roughly be recognized as deep brown (location (b)), brown (location (c)) and limestone white (location (d)). The difference in the extent of the whitening can be attributed to the differences in the mineral components and the conditions of the archaeological environments. With OCT system 2 scanning, the OCT images at the three designated locations are shown in Figures 3 (b)–(d), respectively, and show different depths of backscattering intensity distribution. One can see the deepest distribution in the region of strong whitening (location (d)), similar to the whitened portion in Figure 2 (b). Such observations are particularly clear when compared with the deep brown and brown regions shown in Figures 3 (b) and 3 (c).

Figure 4 (a) shows a photograph of sample C, which is a fragment of archaic jade from the Liangzhu culture site at Tangshan, Yuhang, Zhejian Province (Wang 2002). Its surface and interior have whitened after being deposited underground for 4000–5000 years. With the OCT system 2 scan at the red bar, the OCT image is shown in Figure 4 (b). Here, a typical subsurface structure of a whitened jade object—that is, an almost uniform backscattered intensity distribution—can be seen.

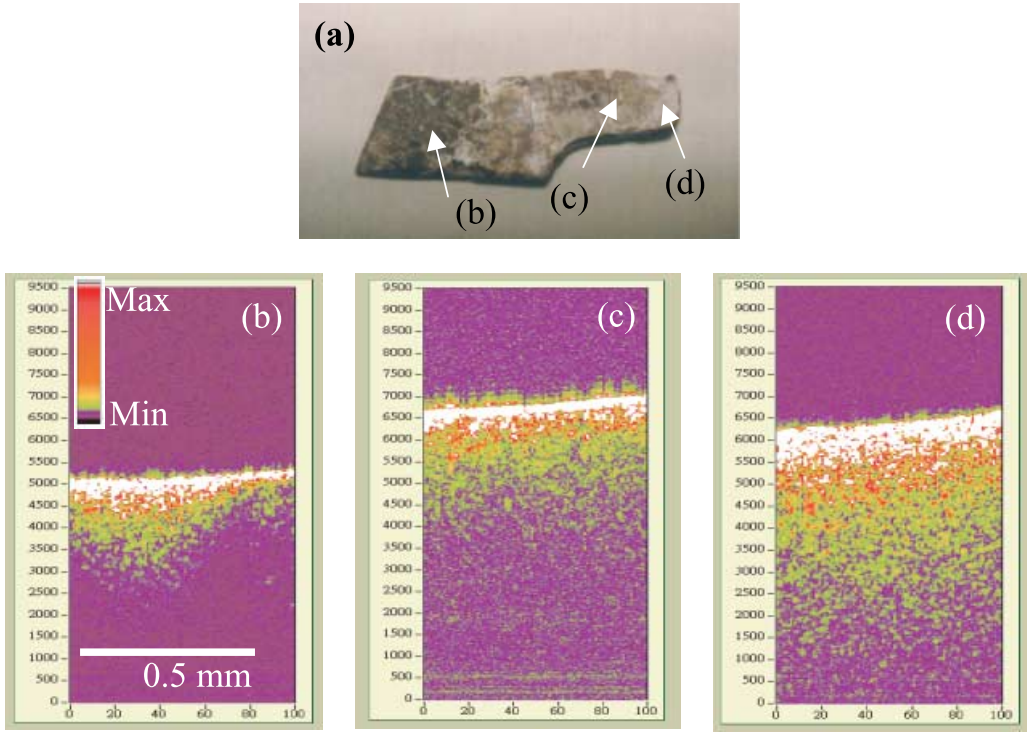

Figure 3 *(a) A photograph of sample B. The OCT scanning images corresponding to the indicated three locations are shown in parts (b), (c) and (d).*

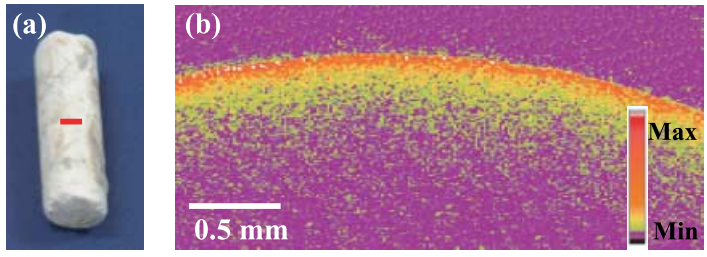

Figure 4 *(a) A photograph of sample C. (b) An OCT scan image of the sample at a location near the red bar in part (a).*

From the OCT scanning results of the three archaic jade objects, we can generally speculate that the whitening process led to subsurface morphologies of higher uniformity in a large scale, but lower uniformity in a small scale. The large and small scales are divided by the spatial resolution of the OCT system, which is in the range of a few microns. In other words, after whitening, the subsurface morphologies of jade objects in the scale of tens of microns or larger disappear. However, the structures in the scale of a few microns or smaller change such that stronger backscattered intensity can be detected. In this situation, the OCT images reveal deeper distributions of backscattered intensity. The shallower distributions of non-whitened jade objects can be attributed to relatively more homogeneous small-scale structures or higher absorption.

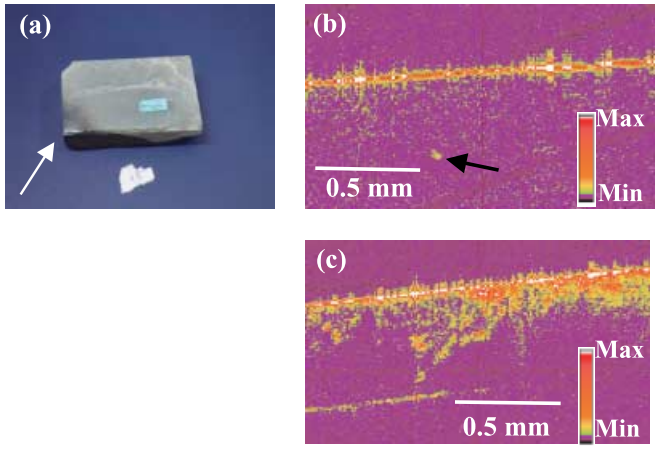

Figure 5 *(a) A photograph of sample D, which is a fresh jade material after burning at the indicated corner. (b) An OCT scan image of the sample at the indicated corner before burning. (c) An OCT scanning image of the sample at the burnt corner, as indicated in part (a).*

A COMPARISON BETWEEN NATURAL WHITENING AND ARTIFICIAL TREATMENT

To understand the differences in subsurface structure between archaic and forged jade objects, we prepared two jade objects and treated them with burning, to imitate the procedure of fabricating a jade forgery. Figure 5 (a) shows a photograph of a fresh piece of nephrite (sample D) with one burnt corner, as indicated by the arrow. Figures 5 (b) and 5 (c) show the OCT scanning images of the sample at the burnt edge before and after burning, respectively. This sample was burned using a gas torch with a temperature of about 1200°C for 15 min. After burning, one can see that the edge of the burnt corner turns white in colour. Before burning, the subsurface structure produces just a few backscattering features. However, the cluster feature, as indicated with the arrow, shows that the light penetration is actually quite deep, which implies that the subsurface structure of this raw material is quite uniform in the small scale, such that backscattering is weak. Note that the stripes (from the upper right to the lower left) represent noise from a low-frequency vibration during measurement. After burning, strong backscattering with features can be observed. It is believed that, after burning, small-scale structures were formed to produce significant backscattering. However, in this process the large-scale structures were preserved or newly generated, as shown in Figure 5 (c). The lower line-feature in Figure 5 (c) denotes the lower surface of the sample near the edge. The results in Figures 5 (b) and 5 (c) provide us with a clue that artificial treatment of jade material, such as burning, may produce the small-scale variations in the subsurface structures. However, the large-scale features are essentially unchanged. This observation may help us to differentiate an archaic jade object from a forged one.

To further explore the subsurface morphologies of sample D before and after burning, we conducted a scanning electron microscopy (SEM) experiment. Figures 6 (a) and 6 (b) show the SEM images of two pieces of sample before and after burning, respectively. The burnt sample was obtained from the burnt corner shown in Figure 5 (a). The unburnt sample was obtained from the other corner. In Figure 6 (a), one can see the structure domain size of a few tens of microns, particularly in the right-hand portion of this image. Within such a domain, the material is essentially uniform. It is speculated that the OCT image in Figure 5 (b) corresponds to a

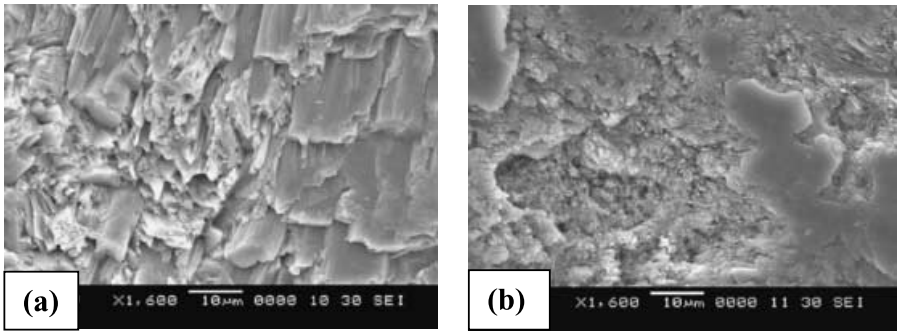

Figure 6 *(a) An SEM image of an unburnt piece of sample D. (b) An SEM image of a burnt piece of sample D at the indicated corner of Figure 5 (a).*

structure like the right-hand portion of Figure 6 (a), which is supposed to be quite transparent. On the other hand, after burning as shown in Figure 6 (b), the small-scale structures, which coexisted with large-scale structures of around 10 μm in size, were generated. The small-scale structures are responsible for the stronger backscattering intensity in Figure 5 (c), in which the large-scale features can also be seen.

Then, we prepared sample E, which is a square tube recently made with fresh material. Three of the sides of the square tube were discoloured by burning. In Figures 7 (a) and 7 (c), we

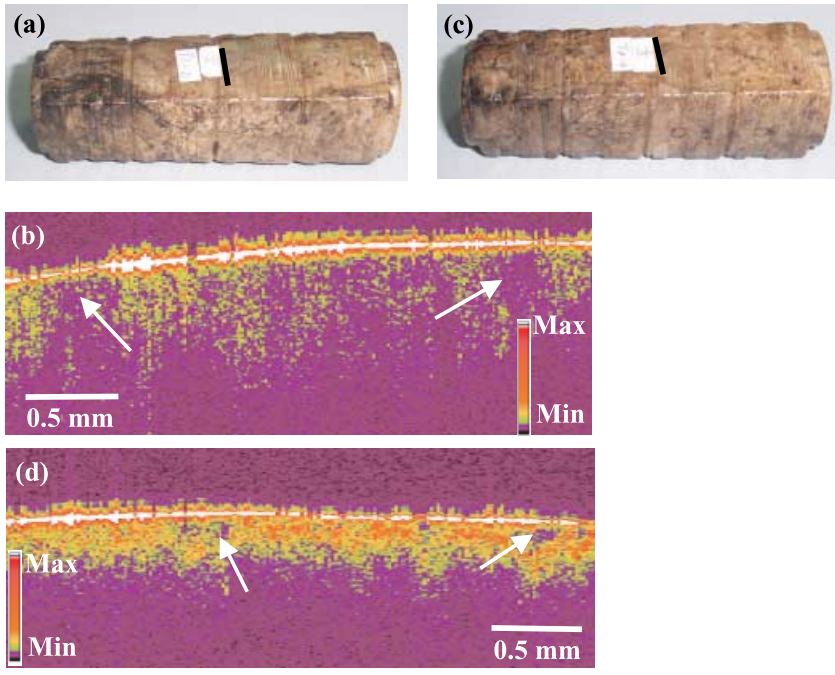

Figure 7 *(a) A photograph of the unburnt side of sample E, which is a recently fabricated jade tube. (b) An OCT scanning image of the unburnt side of the sample at the indicated black bar in part (a). (c) A photograph of two burnt sides of sample E. (d) An OCT scanning image of the burnt side at the indicated black bar in part (c).*

show photographs of the unburnt and burnt surfaces of the sample, respectively, for OCT scanning (scanning at the locations of the black bars). The burning condition for this sample is the same as that of sample D, except that the burning period is only 10 min. After burning, the surface becomes slightly brighter. Figures 7 (b) and 7 (d) show the OCT scanning images (with system 2) of the unburnt and burnt sides, respectively. In the unburnt image, a few features indicated by arrows can be recognized, although the backscattering intensity is not strong. After burning, the backscattering intensity was significantly enhanced. However, just as in the case of Figure 5 (c), the large-scale structures still existed. A few features are indicated by arrows.

From the OCT scanning results shown in this section, we may conclude that after burning, which represents one of the most important procedures in the fabrication of forged jade objects, small-scale structures of sizes beyond the OCT resolution are produced such that the backscattering intensity is enhanced. Meanwhile, the large-scale structures (within the OCT resolution) are preserved or even enhanced. On the other hand, the subsurface morphologies of naturally whitened jades are varied in such a way that small-scale structures are generated and the large-scale ones essentially diminish. Therefore, generally uniform backscattering intensity distributions (decaying with depth) can be observed. Although our OCT scanning for the cases with and without burning cannot be carried out at exactly the same locations on the samples, the above comparisons do provide us a useful method for differentiating archaic jade objects with natural whitening from forged objects produced using burning procedures.

DISCUSSION AND CONCLUSIONS

We have demonstrated the use of the OCT technique for scanning the subsurface morphologies of jade objects. The two-dimensional tomography images were obtained essentially as a result of the refractive index variations in the samples. However, it is believed that material absorption also played an important role. Three samples of archaic jade objects from the Qijia and Liangzhu cultures were scanned in order to understand the subsurface morphologies of the naturally whitened archaic jades. Also, two jade objects with artificial treatments (burning) were scanned and compared with the original materials in subsurface structures. It was found that the subsurface morphologies of the original, artificially treated and naturally whitened objects were quite different. In the original objects, the jade materials could generally be quite transparent, such that the backscattering intensity was weak, although the large-scale (tens of microns or larger) subsurface morphology could be clearly observed. After burning, small-scale (smaller than a few microns) structures were formed and the backscattering intensity was enhanced. In this situation, the large-scale structures might be preserved or even newly generated. Actually, cracks could be produced during the burning process. On the other hand, in an archaic object with natural whitening, small-scale structures were also formed. Hence, deeper distributions of significant backscattering intensity were observed, when compared with the unwhitened objects. Nevertheless, the large-scale features might diminish during the whitening process. With OCT scanning, such differences in subsurface morphology will provide us a valuable reference for authenticating archaic jade objects.

To further develop the OCT technique for such authentication work, several directions are suggested. First, an increase in the scanning depth can definitely provide more useful information. The scanning depth relies on several factors, including material random scattering, absorption and surface morphology. To reduce random scattering in the jade materials, a longer central wavelength of the light source is suggested. This consideration can be combined

with the requirement of reducing absorption in choosing an optimum central wavelength. The search for the optimum wavelength requires an understanding of the absorption spectra of jade materials and consideration of broadband light source availability. Because of the advances in optical fibre communication-related components, a central wavelength of around 1550 nm seems to be a good choice for the next step of development of the method.

The second direction for development is related to the birefringence nature of raw jade materials. Because of the anisotropic structures of jade materials, different polarization components of the incident light experience different refractive indices. Such birefringence characteristics can be explored with the polarization-resolved OCT technique. After the whitening process, the birefringence is expected to be reduced. Therefore, a polarization-resolved OCT system would be more useful for the study of jade (de Boer *et al*. 1999). Meanwhile, since the essential rock subsurface structures are expected to be preserved after an artificial whitening process, a polarization-resolved OCT system can help more in identifying an artificially aged jade object.

Third, to better interpret OCT images of jade objects, more petrographic studies are required. The structures of the jade materials depend on their origins. Different types of jade material may yield different whitening results. Petrographic studies should help us to gain a better understanding of the differences in mineral composition and subsurface morphology between raw materials, naturally whitened objects and artificially treated samples.

Finally, the OCT technique is also useful for the non-invasive scanning of the subsurface morphology of other archaic objects, including lacquer ware and paintings. With the development of OCT systems with a higher resolution, a higher scanning speed, a greater scanning depth and other functions, more archaeological issues can be studied with the assistance of the OCT technique.

ACKNOWLEDGEMENTS

The National Science Council of the Republic of China supported this research under grants NSC 90-2411-H-136-001, NSC 91-2411-H-136-002, NSC 91-2215-E-002-030 and NSC 91-2215-E-002-034.

REFERENCES

Bouma, B. E., Tearney, G. J., Bilinsky, I. P., and Fujimoto, J. G., 1996, Self-phase-modulated Kerr-lens mode-locked Cr:forsterite laser source for Optical Coherence Tomography, *Optics Letters*, **21**, 1839–41.

Chen, Z., Zhao, Y., Srinivas, S. M., and Frostig, R. D., 1999, Optical Doppler tomography, *IEEE Journal of Selected Topics in Quantum Electronics*, **5**, 1134–42.

de Boer, J. F., Milner, T. E., and Nelson, J. S., 1999, Determination of the depth resolved Stokes parameters of light backscattered from turbid media by use of polarization-sensitive optical coherence tomography, *Optics Letters*, **24**, 300–2.

Douglas, J. G., 1996, The study of Chinese archaic jades using non-destructive X-ray fluorescence spectroscopy, *Acta Geologica Taiwanica*, **32**, 43–54.

Fercher, F., Mengedoht, K., and Werner, W., 1988, Eye-length measurement by interferometry with partially coherent light, *Optics Letters*, **13**, 386–8.

Hartl, X., Li, D., and Fujimoto, J. G., 2001, Ultrahigh-resolution optical coherence tomography using continuum generation in an air–silica microstructure optical fiber, *Optics Letters*, **26**, 608–10.

Huang, D., Swanson, E. A., Lin, C. P., Schuman, J. S., and Fujimoto, J. G., 1991, Optical coherence tomography, *Science*, new series, **254**, 1178–81.

Huang, X., 2000, Liangzhu yuqi bianbai chi yanjiu [Study on whitening alternation of jade objects of Liangzhu], *Zhongguo Gudai Yuqi yu Yuwenhua Gaoji Yantaohui* [*Chinese Archaic Jades and Jade Culture Advanced Seminar*], Handout abstracts, 19, Zhongguo Gudai Yuqi yu Yuwenhua Gaoji Yantaohui Choupeichu, Beijing.

Izatt, J. A., Kulkarni, M. D., and Wang, H., 1996, Optical Coherence Tomography and microscopy in gastrointestinal tissues, *IEEE Journal of Selected Topics in Quantum Electronics*, **2**, 1017–27.

Jayne, H. H. F., 1940, Introduction, in *Archaic Chinese jades, special exhibition, February 1940*, 7–11, The University Museum, the University of Pennsylvania, Philadelphia.

Klein, C., and Hurlbut, C. S., Jr., 1999, *Manual of mineralogy*, Ch. 5, 221–49, John Wiley, New York.

Laufer, B., 1912, *Jade: a study in Chinese archaeology and religion*, Field Museum of Natural History, Chicago.

Lin, S. B., Tsien, H. H., and Tan, L. P., 1996, Mineralogical properties and secondary alterations of serpentine archaic jades, *Acta Geologica Taiwanica*, **32**, 149–68.

Loehr, M., and Fitzgerald Huber, L. G., 1975, *Ancient Chinese jades from the Grenville L. Winthrop Collection in the Fogg Art Museum, Harvard University*, Fogg Art Museum, Harvard University, Cambridge, Massachusetts.

Pelliot, P., 1925, *Jades archaiques de Chine appartenant a M. C. T. Loo*, Libraire Nationale d'Art et d'Histoire, Paris.

Renfrew, C., and Bahn, P., 1997, *Archaeology: theories, methods and practice*, Thames and Hudson, New York, 344–5.

Salmony, A., 1938, *Carved jade of ancient China*, Gillick Press, Berkeley, California.

Schmitt, J. M., 1999, Optical Coherence Tomography (OCT): a review, *IEEE Journal of Selected Topics in Quantum Electronics*, **5**, 1205–215.

Tearney, G. J., Bouma, B. E., and Fujimoto, J. G., 1997, High-speed phase- and group-delay scanning with a grating-based phase control delay line, *Optics Letters*, **22**, 1811–13.

Tsien, H. H., and Tan, L. P., 1998, *Zhongguo guyujian: zhizo fangfa ji kuanwu jianding* [*The connoisseur of Chinese jade: manufacturing methods and geological appraisal*], Diqui chubanshe, Taiwan.

Wang, M., 2002, Tangshan yizhi faxian Liangzhu wehua zhiyu zofang [The finding of a jade manufactory at the Tanshan site of the Liangzhu culture], *Zhongguo Wenwubao*, no. 1049, 20 September, 1.

Wen, G., 1992, Bienyu [Discussing jades], *Wenwu*, **7**, 75–9.

Wen, G., 1993, Zhongguo guyu dizhi kaoguxue yanjiu ti xuchinzhan [Continuing geo-archaeological studies on Chinese archaic jades], *Gugong Xueshu Jikan*, **11**(1), 9–29.

Wen, G., 1994a, Guyu di shouqin [Secondary alternation of archaic jade], *Gugung Wenwu Yuekan*, **11**(12), 92–101.

Wen, G., 1994b, Jigubai yu xiangyabai guyu [Chicken bone white and ivory white of archaic jades], *Gugung Wenwu Yuekan*, **12**(2), 116–29.

Wen, G., 1998, Some characteristics of prehistoric jades from mainland China, *East Asian Jade: Symbol of Excellence*, **2**, 217–21, Center for Chinese Archaeology and Art, The Chinese University of Hong Kong, Hong Kong.

Wen, G., and Jing, Z., 1996, Mineralogical studies of Chinese archaic jade, *Acta Geologica Taiwanica*, **32**, 55–83.

Xu, J., Huang, E., Chen, C., Tan, L., and Yu, B., 1996, A Raman spectroscopic study of archaic jades, *Acta Geologica Taiwanica*, **32**, 11–42.

Yang, M., 2000, The three topics on the jade objects of the Liangzhu culture, in *Presentation for the Workshop on the Purchased Jade Objects in the Last Six Years in the National Palace Museum*, National Palace Museum, Taipei.

Zheng, J., 1983, Jiang-su Wu-xian xinshiqi shidai izhi chutu di guyu yanjiu [Studies on archaic jade of the Neolithic period unearthed in Wu County, Zhejian Province], *Kaoguxue Jikan*, **3**, 218–24.

Zheng, J., 1986, Wuxian Zhanglinshan Dongshan yizhi chutu yuqi jianding baogao [Appraisal report on excavated jade objects of Tongshan Mountain, Zhanglingshan Mountain, Wu County], *Wenwu*, **10**, 39–41.